OGG1 protects mouse spermatogonial stem cells from reactive oxygen species in culture[1]

Yoshifumi Mori[2], Narumi Ogonuki[3], Ayumi Hasegawa[3], Mito Kanatsu-Shinohara[2], Atsuo Ogura[3], Yufeng Wang[4], John R. McCarrey[4] and Takashi Shinohara[2]

[2]Department of Molecular Genetics, Graduate School of Medicine, Kyoto University, Kyoto 606-8503, Japan
[3]RIKEN, BioResource Research Center, Tsukuba 305-0074, Japan
[4]Department of Biology, University of Texas at San Antonio, San Antonio, TX 78249, USA

Address correspondence and reprint requests to: Takashi Shinohara, Department of Molecular Genetics, Graduate School of Medicine, Kyoto University
Yoshida Konoe, Sakyo, Kyoto 606-8501, Japan
Tel: 81-75-751-4160; Fax: 81-75-751-4169; E-mail: tshinoha@virus.kyoto-u.ac.jp

Running title: ROS resistance by OGG1
One sentence summary: OGG1 suppresses ROS-induced damages in spermatogonial stem cells.

[1]Financial support for this research was provided by The Uehara Memorial Foundation, and The Ministry of Education, Culture, Sports, Science, and Technology of Japan (18H05281).

Abstract

Although reactive oxygen species (ROS) are required for spermatogonial stem cell (SSC) self-renewal, they induce DNA damage and are harmful to SSCs. However, little is known about how SSCs protect their genome during self-renewal. Here we report that *Ogg1* is essential for SSC protection against ROS. While cultured SSCs exhibited homologous recombination-based DNA double-strand break repair at levels comparable to those in pluripotent stem cells, they were significantly more resistant to hydrogen peroxide than pluripotent stem cells or mouse embryonic fibroblasts, suggesting that they exhibit high levels of base excision repair (BER) activity. Consistent with this observation, cultured SSCs showed significantly lower levels of point mutations than somatic cells, and showed strong expression of BER-related genes. Functional screening revealed that *Ogg1* depletion significantly impairs survival of cultured SSCs upon hydrogen peroxide exposure. Thus, our results suggest increased expression of BER-related genes, including *Ogg1*, protects SSCs from ROS-induced damage.

Introduction

DNA repair of self-renewing tissues is an important topic because any defects in stem cells are transmitted to their progenitor cells and influence the tissue turnover and function [1]. When DNA lesions directly impair self-renewal, the tissue will be depleted of stem cells and will fail to function properly due to a lack of mature differentiated cells. Even a subtle difference in the self-renewal rate can be deleterious because stem cells in many tissues compete against each other for their optimal microenvironment. DNA mutations in the germline are particularly critical because they not only lead to infertility but also generate de novo mutations that may give rise to new diseases in the next generation. Five percent of live-born human offspring have a genetic disorder and 20% of these disorders are caused by de novo mutations [2]. Compared to female germline cells, male ones undergo extensive replication before gamete production, which has the potential to generate more mutations in the male-derived genome [3]. To counter this potential dilemma, it is likely that germ cells possess a unique DNA repair system that mitigates the accumulation of de novo point mutations.

Studies of male germ cells have been hampered by difficulties in introducing genetic manipulation. However, an exception has been spermatogonial stem cells (SSCs). SSCs divide continuously to sustain spermatogenesis throughout the life of male animals [4,5]. Indeed, they are thought to comprise only 0.02-0.03% of total germ cells in the testis [5,6]. Despite their small number, SSCs can be expanded in vitro by their self-renewal activity. With supplementation of SSC self-renewal factors, such as GDNF and FGF2, grape-like clusters of spermatogonia can proliferate in vitro for > 2 years [7]. These

78 cells, designated as germline stem (GS) cells, can reinitiate spermatogenesis upon
79 transplantation into the seminiferous tubules of infertile animals. Although the frequency
80 of SSCs in GS cell cultures is low (~1-2%), this culture system allows the in vitro
81 expansion and genetic manipulation of SSCs, facilitating biochemical and molecular
82 analyses of the male germline [8]. Thus, using GS cells, we previously showed that
83 reactive oxygen species (ROS) drive SSC self-renewal [9]. NOX1 is a major producer of
84 ROS and mice deficient in *Nox1* exhibit impaired self-renewal in vivo, whereas
85 supplementation of H_2O_2 enhances GS cell proliferation in vitro. Deletion or depletion of
86 genes involved in ROS generation, such as *Mapk14* or *Mapk7*, impairs GS cell
87 proliferation and induces apoptosis [10].

88 However, ROS also induce DNA damage. DNA double-strand breaks (DSBs)
89 are the most severe type of damage and are lethal and oncogenic. DSBs are repaired by
90 non-homologous end-joining (NHEJ) or homologous recombination (HR)[11]. HR is an
91 error-free repair process that occurs most efficiently in the late S and G2 phases of the
92 cell cycle because HR demands homologous strands to serve as an original template for
93 correcting damaged DNA. On the other hand, NHEJ occurs throughout the cell cycle but
94 is prone to error. ROS also induce other forms of DNA damage through oxidization of
95 nucleotide bases. 8-oxoguanine (8-OxoG) is one of the most common DNA lesions
96 caused by oxidative stress [12]. The lesion results in G:C to T:A transversions. Oxidized
97 bases are typically repaired by the base excision repair (BER) pathway, but when they
98 occur simultaneously on opposing strands, attempted BER can lead to the generation of

DSBs. To ensure pristine genome preservation, SSCs must correct these mutations as precisely as possible during self-renewal.

Several in vivo studies have suggested that male germ cells possess a unique DNA repair machinery. For example, morphological analyses of irradiated testes have shown that ZBTB16^{+} spermatogonia lack histone-associated signaling components of the DNA repair machinery, such as γH2AX/MDC1, which are recruited immediately to DSBs after damage in somatic cells [13]. Male germ cells also undergo dynamic changes in DNA mutation frequency. A series of studies that used *LacI* mutation-reporter mice ("Big Blue mice") showed that the estimated point mutation frequencies of a mixed population of spermatogenic cells are lower than those in somatic cells [14]. Closer examination revealed a decline in mutation frequency during spermatogenesis, such that the mutation frequencies in type B spermatogonia and all subsequent stages of spermatogenesis were lower than the frequency in primitive type A spermatogonia [2]. In addition, spermatogenic cells from old mice showed significantly higher mutation frequencies than those from young mice [2]. Therefore, DNA repair and mutation frequency in spermatogenic cells change according to their differentiation status and age. More recent studies have suggested that the numbers of DNA mutation frequencies in embryonic stem (ES) cells, induced pluripotent stem cells and spermatogonia are very low compared to somatic cells [15,16], which suggested high levels of BER activity in these cells. Although these results suggest a similarity between pluripotent stem cells and spermatogonia, GS cells are significantly more sensitive to irradiation than ES cells [17]. While ES cells continue to proliferate after irradiation [18], GS cells undergo apoptosis

121 at significantly lower radiation doses. These results suggest that SSCs have a unique DNA
122 repair machinery not found in ES cells or somatic cells.
123 In this study, we sought to understand the mechanism by which GS cells tolerate
124 ROS. We evaluated the DSB repair machinery by transfecting DNA substrates into GS
125 cells and determined the contributions of NHEJ and HR. We found that the expression of
126 genes involved in BER is up-regulated in GS cells relative to other cell types and revealed
127 that *Ogg1* is responsible for protecting GS cells from ROS.
128
129 **Materials and Methods**
130 *Animals*
131 The Big Blue mice were obtained from Taconic Farms, Inc. (Hudson, NY).
132 These mice were maintained in a C57BL/6 (B6) background. The Institutional Animal
133 Care and Use Committee of Kyoto University approved all animal experimentation
134 protocols.
135
136 *Cell culture*
137 For GS cell cultures, wild-type (WT) and *Trp53* knockout (KO) GS cells in an
138 ICR background were previously described [19]. We also derived GS cells from Big Blue
139 mice (B6 × DBA/2 F1; BDF1). These cells were derived from 2-8 days old pups. For
140 experiments using multipotent germline stem (mGS) cells from Big Blue mice, mGS cells
141 were induced by suppressing *Dmrt1* and *Trp53* in GS cells, as previously described [20].
142 ES cells (R1) were a generous gift from Dr. M. Ikawa (Osaka University, Osaka, Japan).

Mouse embryonic fibroblasts (MEFs) were prepared from 13.5 days post-coitum ICR or Big Blue mouse BDF1 embryos. Tail tip fibroblasts (TTFs) were collected from adult Big Blue mice. GS cells were maintained on MEFs using Iscove's modified Dulbecco's medium supplemented with GDNF and FGF2, as described previously [21]. ES cells and mGS cells were maintained on MEFs using Dulbecco's modified Eagles's medium (DMEM) supplemented with 15% fetal bovine serum (FBS), 1000 U/ml leukemia inhibitory factor (ESGRO; Merck Millipore, Darmstadt, Germany), nonessential amino acid mixture (Invitrogen, Carlsbad, CA), 0.1 mM 2-mercaptoethanol (2-ME), 2 μM PD0325901 (Selleck Chemicals, Houston, TX), and 3 μM CHIR99021 (Biovision, Milpitas, CA). MEFs and TTFs were cultured in DMEM supplemented with 10% FBS. Where indicated, culture medium was supplemented with H_2O_2 (Wako, Kyoto, Japan).

Virus transfection

The lentiviral knockdown (KD) vectors used in the present study were purchased from Open Biosystems (Huntsville, AL), and pLKO1-Scramble shRNA was used as a control (Addgene, Cambridge, MA). For overexpression of cDNAs, mouse *Ogg1* was cloned into CSII-EF-IRES-puro (RIKEN Bioresource Center, Tsukuba, Japan). Lentivirus transfection was performed as described previously [9]. Multiplicity of infection (MOI) was adjusted to 10.0 and 1.0 for lentivirus infection. All KD vectors are listed in Supplemental Table S1.

Immunostaining

Testes were fixed in 4% paraformaldehyde for 2 h at 4°C before embedding in Tissue-Tek OCT compound (Sakura Finetek, Tokyo, Japan) for cryosectioning. Then sections of 4 μm thickness were prepared and slides were incubated in 0.1% Triton X-100. For staining of GS cells, cells were dissociated using trypsin, and single cell suspensions were concentrated on glass slides by centrifugation using a Cytospin 4 unit (Thermo Elecron Corp, Cheshire, UK). The slides were incubated in 0.01% Triton-X for 15 min for permeabilization. After immersion of slides in the blocking buffer [0.1% Tween 20, 1% bovine serum albumin (BSA) and 10% normal donkey serum in phosphate-buffered saline (PBS)], samples were incubated with indicated antibodies or rhodamine-labeled PNA (Vector Laboratories, Burlingame, CA). OGG1 levels were quantified using the MetaMorph software (Molecular Devices, Sunnyvale, CA). Cells were counterstained with Hoechst 33342 (Sigma, St. Louis, MO). The antibodies used are listed in Supplemental Table S2.

Alkaline comet assay

The alkaline comet assay was performed as described previously [22]. In brief, cells were incubated with H_2O_2 for 30 min on ice followed by the incubation in their respective culture medium at 37°C for the indicated periods of time. After centrifugation, cells were embedded in 0.75% low-gelling temperature agarose (A4018; Sigma) on poly-L-lysine-coated glass slides (Matsunami Glass, Osaka, Japan). Then the cells were lysed by incubating the slides at 4°C in lysis buffer [1% Triton X-100, 0.5% N-Lauroryl sarcosine sodium salt, 2.5 M NaCl, 100 mM EDTA (pH 8.0), and 10 mM Tris-HCl (pH

10.0)]. After washing twice in PBS, the slides were immersed in pre-chilled electrophoresis buffer (0.3 M NaOH and 1 mM EDTA in water) for 40 min and electrophoresis was performed at 25 V for 50 min at 4°C. Then the samples were washed twice in 400 mM Tris-HCl (pH 7.0) at room temperature and soaked in ethanol for 5 min, followed by overnight drying at 37°C. DNA was detected by ethidium bromide staining for 30 min at room temperature. After rinsing in PBS, slides were observed via confocal microscopy and quantified using the Metamorph software.

Terminal deoxynucleotidyl transferase dUTP nick end labeling (TUNEL) staining

Apoptotic cells were detected using the in situ cell death detection kit: TMR red (Roche Applied Science, Mannheim, Germany) according to the manufacturer's instructions. Cells were counterstained using Hoechst 33342.

Gene expression analyses

Total RNA was isolated using TRIzol (Invitrogen). For real-time polymerase chain reaction (PCR), first-strand cDNA was produced using a Verso cDNA synthesis kit. Real-time PCR was performed using StepOnePlus™ real-time PCR system (Applied Biosystems, Cheshire, UK) and the *Power* SYBR Green PCR Master Mix (Applied Biosystems). Transcript levels were normalized against *Hprt* expression. The PCR conditions were as follows: 95°C for 10 min, followed by 40 cycles at 95°C for 15 s and 60°C for 1 min. Each PCR experiment was performed in triplicates. PCR primers are listed in Supplemental Table S3.

209

210 *Analyses of mutation frequency by Big Blue mice*

211 The Big Blue mouse assay was performed as described previously [16]. In brief,
212 genomic DNA collected from experimental samples was used to recover the lambda
213 shuttle vector containing the *LacI* mutation-reporter gene according to the manufacturer's
214 instructions (Stratagene; La Jolla, CA). SCS-8 *E coli* strain cells were mixed with the
215 packaged phage and plated at < 17,500 plaque-forming units per 25 × 25 cm NZY agar
216 assay tray (Stratagene). Plates were incubated at 37°C for 16-18 h, and stained by
217 incubating with X-gal to detect mutant plaques. The *LacI* gene was amplified by PCR
218 from DNA samples recovered from the mutant phages. The gene sequence of the mutant
219 *LacI* gene was compared with that of the WT *LacI* gene to a) confirm the presence of a
220 mutation, b) determine the spectrum of mutations detected in each sample, and c) identify
221 and adjust for any clonal mutants (= the same mutation at the same location in the *LacI*
222 gene in more than one mutant phage plaque). Numbers of mutations were analyzed by a
223 Poisson model with parameter estimates obtained by the method of maximum likelihood
224 [23]. Because of the low expected frequencies, exact p-values were calculated by the
225 exact conditional test for Poisson variables to compare differences between mutation
226 frequencies, using the Exactci package implemented in R [24,25].

227

228 *Magnetic cell sorting (MACS)*

229 Testis cells from Big Blue mice were dissociated using 1 mg/ml collagenase
230 type II for 10 min (Sigma) and dissociated into single cells by repeated pipetting, as

231 described previously [26]. The dissociated cells were incubated with anti-CDH1 antibody
232 for 10 min (ECCD2; a gift from Dr. M. Takeichi, RIKEN CDB, Kobe, Japan). The cells
233 were washed twice with PBS supplemented with 1% FBS, and anti-rat IgG magnetic
234 beads were added and incubated for 15 min on ice (Miltenyi, Aubum, CA). Magnetic cell
235 sorting was carried out as using Miltenyi large cell column.
236
237 *NHEJ assay*
238 The NHEJ assay was performed as described previously [27]. In brief, GS cells
239 were electroporated with pJH200, *Rag1*, and *Rag2*-expression plasmids using the Neon
240 Transfection System (Thermo Fisher Scientific, Waltham). The survival rate was
241 measured by trypan blue staining. The extrachromosomal plasmids were collected from
242 the transfected cells after 48 h using a modified Hirt extraction method [28], which was
243 used to transform competent DH5α *E. Coli* cells. Transformed bacteria were plated on
244 LB-agar containing 100 μg/ml ampicillin (Amp) and/or 5 μg/ml chloramphenicol (Cm;
245 both from Wako), and incubated for 24 h at 37°C.
246
247 *HR assay*
248 The HR assay was performed as described previously [29,30]. In brief, GS or
249 ES cells were electroporated with pHPRT-DRGFP (gift from Dr. M. Jasin; Sloan
250 Kettering Institute, New York, NY) using the Neon Transfection System (Thermo Fisher
251 Scientific) and stable clones were obtained by puromycin selection and confirmed by
252 Southern blotting. To assay green fluorescent protein (GFP) expression, cells were

253 transfected with pSce-I endonuclease (Addgene), and the pCAG-DsRed reporter by
254 lipofectamine 3000 (Thermo Fisher Scientific). Transfection efficiency was estimated by
255 quantifying DsRed fluorescence by FACSCalibur (BD Bioscience, Frankin Lakes, CA).
256
257 *Statistical analyses*
258 Results are presented as the means ± SEM. Data were analyzed using the
259 Student's *t*-tests. Multiple comparison analyses were performed using ANOVA followed
260 by Tukey's HSD test.
261
262 **Results**
263 *Increased survival of GS cells against H_2O_2*
264 We previously showed that ROS are required for GS cell proliferation [9]. To
265 compare the sensitivity of GS cells with other cell types, we used ES cells, mGS cells, a
266 pluripotent cell type derived from GS cells [19], and MEFs. These cells were cultured in
267 the presence of H_2O_2 (10 μM to 1 mM), which is permeable through the cell membrane.
268 Although exposure to high concentrations of H_2O_2 killed GS cells (> 500 μM), low
269 concentrations of H_2O_2 promoted GS cell proliferation without apparent damage (Fig. 1A,
270 B). This enhancement of proliferation is consistent with a previous study [9]. However,
271 H_2O_2 induced extensive apoptosis of other cell types even at 10 μM. The number of
272 apoptotic cells increased in a dose-dependent manner. When TUNEL staining was carried
273 out at 50 μM, significantly enhanced apoptosis was evident (Fig. 1C). In particular, MEFs
274 showed the most severe response. Because apoptosis from irradiation can be attenuated

by *Trp53* deficiency in GS cells [17], we investigated the impact of *Trp53* on H_2O_2-induced apoptosis at 500 μM. As expected, loss of *Trp53* increased cell recovery, and significantly reduced the number of $TUNEL^+$ cells (Supplemental Fig. S1A, B), which suggests that *Trp53* is involved in ROS-induced GS cell apoptosis.

To quantify DNA damage, we performed an alkaline comet assay [31], which detects both single-strand breaks (SSBs) and DSBs, and measured the length of the DNA tail. Although GS cells showed enhanced proliferation at 50 μM H_2O_2 (Fig. 1B), they also showed DNA damage at this concentration, which was quickly recovered after 10 min. MEFs showed a more significant increase in the DNA fraction that migrated into the comet tail even at 10 μM (Fig. 1D). However, all cell types showed significant recovery after 30 min. GS cells also showed extensive damage at 500 μM H_2O_2, but also recovered efficiently. These results suggest that GS cells are more resistant to ROS than other cell types.

Analyses of DSB repair machinery in GS cells

DSBs represent major damage caused by high concentrations of H_2O_2. Previous studies have shown that H_2O_2 (10-100 μM) can induce chromosome damage in primary skin cells of mice [32]. To understand the mechanism of H_2O_2 resistance, we first analyzed the expression of genes involved in DSB repair. DSBs are repaired by NHEJ or HR pathways. Using real-time PCR, we examined the expression of *Xlf* (NHEJ), *Xrcc6* (NHEJ), *Brca1* (HR), and *Rad51* (HR). We found stronger expression of all of these genes

296 in GS cells than in other cell types (Fig. 2A). Some, but not all of these genes were
297 influenced by supplementation of H_2O_2 (Supplemental Fig. S2).

298 To directly examine the type of DSB repair in a functional manner, we next
299 carried out a series of transfection experiments to test NHEJ activity using pJH200 (Fig.
300 2B). This plasmid contains two heptamer-nonamer immunoglobulin-joining signal
301 sequences flanking a prokaryotic transcription terminator, which prevents expression of
302 the Cm-resistant genes [27]. Signal sequence removal by *Rag1* and *Rag2* recombinase
303 gene transfection allowed Cm-resistant gene expression. Based on the previous
304 experiments using lymphocytes [27], we transfected pJH200 substrate vector into GS
305 cells. The viability of cells after transfection, as estimated by trypan blue staining, was
306 31.0 ± 4.2%, 34.4 ± 4.1%, 32.8 ± 3.8%, and 82.8 ± 2.5%, respectively, for GS cells. ES
307 cells, mGS cells, and MEFs, respectively (n = 4). The substrate plasmid was recovered 2
308 days after transfection and introduced into *E. coli* before plating on LB agar plates
309 containing either Amp or Amp/Cm. When the ratio of successful recombination was
310 quantified by measuring the number of Cm-resistant colonies and Amp-resistant colonies,
311 we found that MEFs had significantly elevated NHEJ activity compared to other cell
312 types (Fig. 2C). This is consistent with previous studies that have found that somatic cells,
313 but not ES cells, use NHEJ predominantly to repair DSBs [33]. We did not find statistical
314 significance in levels of NHEJ among the other cell types.

315 We next compared HR activity using pHPRT-DRGFP, which contains two GFP
316 cassettes: a nonfunctional mutant GFP, SceGFP, engineered to contain an 18-bp
317 restriction site for the endonuclease Sce-I, and an internal GFP, which contains a 5'- and

318 3’-truncated fragment capable of correcting the mutation in the SceGFP cassette.
319 Transfection of Sce-I into cells that contain pHPRT-DRGFP induces a DSB, which can
320 be corrected with GFP by HR, as described previously (Fig. 2D)[29]. Using this system,
321 we focused on GS cells and ES cells because these cells did not show significant
322 differences in the NHEJ activity. Because this assay depended on analysis of stably
323 transfected cells, we were not able to analyze MEFs, which undergo senescence during
324 repeated passages. We found a significant increase in GFP expression in both GS cells
325 and ES cells after transfection of the Sce-I-expressing plasmid (Fig. 2E). However, no
326 significant differences in GFP fluorescence were seen between the two cell types. These
327 results suggest that GS cells and ES cells have comparable levels of HR-based DNA
328 repair activity in restoring GFP expression.
329
330 *Quantification of DNA mutations using Big Blue mice*
331 Although our results suggest that GS cells use HR to survive H_2O_2 treatment,
332 the experiment in the preceding section could not explain the difference between ES and
333 GS cells. However, H_2O_2 can cause several types of DNA damage. DSBs constitute the
334 most severe types of damage, but H_2O_2 also induces point mutations, which are corrected
335 by BER [12]. Considering their strong resistance to ROS and previous studies regarding
336 the high BER activity of male germ cells [34], we speculated that GS cells exhibit a strong
337 BER capacity. Indeed, freshly collected spermatogonia are reported to have a low point
338 mutation frequency compared to somatic cells [16]. However, because cell proliferation
339 decreases BER activity in some cell types [35,36], we analyzed whether GS cells maintain

the low mutation frequency phenotype. For this experiment, we used Big Blue mice (Fig. 3A). These mice contained the prokaryotic *LacI* gene as a mutation reporter transgene. This transgene can be recovered from any cell type and cloned into a lambda shuttle vector, which can be packaged into a phage that can infect *E. coli* host cells. If any inactivating mutation arises in the *LacI* transgene, repression of the *Lac* operon will cease, allowing beta galactosidase to be produced from the *E. coli*, which can be detected by adding X-gal to the plating medium.

In this experiment, we derived GS cells from Big Blue mice. We also collected $CDH1^+$ undifferentiated spermatogonia from mice 8- to 10-months old by MACS and compared their mutation frequencies. Flow cytometic analysis of CDH1-selected cells showed that $CDH1^+$ cells comprise 24.0 ± 2.0% (n = 4)(Supplemental Fig. S3). For analyses of GS cells, cells from two different time points (8 and 31 months after culture initiation) were analyzed. This was because we were interested to study the impact of in vitro aging. We also used mGS cells as a pluripotent cell type. MEFs and TTFs were used as somatic cell controls. Overall, quantification of mutation frequency revealed that GS cells exhibited relatively low mutation frequencies among the different cell types (Fig. 3B). $CDH1^+$ spermatogonia or mGS cells also showed a lower frequency than MEFs or TTFs, consistent with the results of a previous study [16]. The difference between 31 months old GS cells (31M-GS cells) and MEFs (p = 2.74E-05) or TTFs (p = 7.06E-09) were statistically significant. In contrast, we did not find statistical difference between 31M-GS cells and $CDH1^+$ spermatogonia (p = 0.13), mGS cells (p = 0.24) or 10M-GS cells (p = 0.61). Sequencing of *LacI* mutants showed both transversions and transitions

362 in all cell types (Supplemental Table S4). These results suggest that GS cells similarly
363 maintain a low point mutation frequency, similar to that found in freshly prepared
364 spermatogonia.
365
366 *Expression of BER-related genes in GS cells*
367 To study the mechanism of the low point mutation frequency in GS cells, we
368 performed real-time PCR and examined expression of BER-related genes in GS cells, ES
369 cells, mGS cells, and MEFs. The BER-related genes include *Apex1*, *Ercc6*, *Fen1*, *Mbd4*,
370 *Mth1*, *Mutyh*, *Neil1*, *Ogg1*, *Pnkp*, *Rpa1-3*, *Tdg*, *Ung*, and *Xrcc1*. These genes were
371 selected based on the previous publications that showed their functional involvement in
372 BER [37-40]. The lack of these genes can cause various defects. For example, deletion of
373 *Ercc6*, *Mbd4*, *Ogg1*, *Mutyh*, *Neil1*, *Rpa1-3* or *Ung* increases the risk of neoplasm, while
374 *Apex1* or *Tdg* deficiency results in embryonic lethality [37-40]. Of the 15 genes that were
375 examined, 11 genes were most strongly expressed in GS cells (Fig. 4A). To study the
376 impact of BER-related genes in a functional manner, we transfected lentiviruses that
377 expressed short hairpin RNA (shRNA) against each BER-related gene (Supplemental Fig.
378 S4). Cell recovery showed a significant decrease in GS cell number after depletion of
379 *Ogg1* (Fig. 4B). *Ogg1* is also one of the genes that were influenced by H_2O_2
380 (Supplemental Fig. S2). OGG1 is responsible for the removal of oxidized base. It
381 recognizes the damaged base and excises it from the DNA strand. *Ogg1* can control
382 transcription factor homing, induce allosteric transition of G-quadruplex structure, or
383 recruit chromatin remodelers [41, 42]. Because ROS are constantly generated during GS

384 cell proliferation [10], these results raised a possibility that *Ogg1* is responsible for
385 protecting GS cells from ROS damage.

386 Western blotting showed that OGG1 is expressed more strongly in GS cells
387 than in other cell types (Fig. 4C). However, immunostaining of WT testis showed that
388 OGG1 expression was not specific to spermatogonia (Fig. 4D). It was found not only in
389 the nucleus, but also in the cytoplasm. The cytoplasmic localization of OGG1 may reflect
390 its function in the mitochondrial DNA repair [42]. Compared to $GFRA1^{+}$ undifferentiated
391 spermatogonia, the number of cells expressing OGG1 slightly but significantly increased
392 during differentiation of spermatogonia into spermatocytes, while its expression
393 decreased significantly in peanut agglutinin (PNA)-reactive haploid cells. The increased
394 expression of OGG1 in spermatocytes and round spermatids was previously noted and
395 suggested that OGG1 is involved in progression of meiosis [43]. OGG1 is not specific to
396 germ cells because Sertoli cells are also immunoreactive to the antibody.

397 We then tested the function of OGG1 on GS cells upon H_2O_2 treatment. We
398 first used a comet assay to examine its function on DNA damage. Our analysis showed
399 that *Ogg1* KD decreased the head/total DNA ratio, while overexpression (OE) of *Ogg1*
400 resulted in the opposite effect, which suggests that *Ogg1* expression levels are closely
401 correlated with the level of DNA damage in GS cells (Fig. 5A). In the second set of
402 experiments, we tested the function of *Ogg1* KD or OE on GS cell proliferation in the
403 presence of H_2O_2 (Fig. 5B). As expected, cell recovery after culture was significantly
404 reduced by *Ogg1* KD (Fig. 5C). However, *Ogg1* OE did not improved survival of
405 transfected cells.

To understand the mechanism of OGG1-mediated protection from ROS, we first analyzed whether *Ogg1* OE or KD might change the expression levels of genes involved in DNA repair. However, real-time PCR analysis did not show strong impact on their expression levels (Supplemental Fig. S5). We then performed immunostaining. Although OGG1 was predominantly found in the cytoplasm of GS cells under normal culture conditions, it moved to the nucleus upon H_2O_2 exposure (Fig. 5D), consistent with the previous observation that relocalization of OGG1 initiates DNA repair [37]. Taken together, these results suggest that *Ogg1* plays a critical role in preventing H_2O_2-induced DNA damage in GS cells.

Discussion

We investigated how SSCs protect their genome from ROS, which are essential for self-renewal division. ROS-mediated self-renewal in SSCs is counterintuitive because ROS induce DNA mutations and genetic instability. Our initial analysis revealed that GS cells are significantly more resistant to H_2O_2 than pluripotent stem cells or MEFs. We did not expect this result because ES and mGS cells are significantly resistant to irradiation than GS cells [17]. In that experiment, GS cells were arrested at the G1 phase of the cell cycle and many cells underwent rapid apoptosis, while ES and mGS cells did not show apparent changes. Indeed, γH2AX staining persisted longer in GS cells, which suggested that DSB repair is relatively slower in GS cells [17]. This slow DSB repair was in sharp contrast to rapid recovery of DNA damage after H_2O_2 exposure.

427 We initially thought that GS cells and ES cells are similar in their DNA repair
428 machinery because both cell types allow gene targeting by HR [44-46]. DSBs are
429 predominantly repaired by the NHEJ pathway in higher eukaryotes [13], including MEFs
430 and tissue-specific stem cells, such as hematopoietic stem cells (HSCs) and neural stem
431 cells (NSCs) [1,47,48]. In this sense, ES or GS cells are unique that they can use HR for
432 DSB repair. This may be why gene targeting is feasible in ES or GS cells. Because germ
433 cells transmit genetic information to the next generation, it is reasonable that they
434 preferentially use more precise HR to repair DNA damage to minimize replicative errors.
435 However, because the HR efficiency was comparable between ES and GS cells, this
436 activity alone probably does not explain the high survival rate of GS cells after H_2O_2
437 exposure.

438 We next checked BER activity because ROS also induce point mutations.
439 Although male germline cells show modest nucleotide excision repair and DSB repair
440 activities [49,50], they exhibit elevated levels of BER activity [51]. However, it has not
441 been easy to test the BER activity of SSCs or undifferentiated spermatogonia because
442 they comprise a small population in total testis germ cells. We overcame this problem
443 using GS cells because it is possible to collect a large number of SSCs. However, because
444 in vitro culture might change their property, we examined the mutation frequency of GS
445 cells from Big Blue mouse, which were previously used to demonstrate low mutation
446 frequency in freshly isolated spermatogonia [16]. This analysis revealed that GS cells
447 from Big Blue mice still maintained a low mutation frequency. When compared to TTFs
448 or MEFs, mutation frequencies were lower in fully established GS cells ($0.41\text{-}0.69 \times 10^{-}$

449 ^{5}). These values were comparable to those found in THY1^{+} spermatogonia (0.59×10^{-5}),
450 but were lower than those found in spermatogonia of 6-day-old pup testes (2.34×10^{-5})
451 or prospermatogonia in 15-day-old embryos (0.99×10^{-5}) in a previous study [16].
452 Although CDH1^{+} spermatogonia (1.93×10^{-5}) showed relatively high mutation
453 frequencies, this was probably due to contamination by somatic cells, which is inevitable
454 during MACS-mediated cell recovery. These results confirm previous observations of
455 high BER activity in male germ cells and suggest that GS cells can be used to analyze
456 factors involved in high BER activities.

457 Because ES cells also have a lower point mutation frequency than somatic cells
458 [33], it was possible that difference in the BER activity explains the ROS resistance. To
459 test this hypothesis directly, we examined the expression of BER-related genes in various
460 cell types. As we expected, many BER-related genes are expressed in GS cells compared
461 with other cell types. Through functional screening of BER-related genes, we eventually
462 found that *Ogg1* depletion significantly impaired the survival of GS cells. *Ogg1* is a DNA
463 glycosylate enzyme that is responsible for the excision of 8-OxoG [52]. We further
464 confirmed the involvement of *Ogg1* in ROS protection against H_2O_2 (Fig. 5A). Although
465 OGG1 was relatively widely expressed in the testis, its strong expression in GS cells and
466 our functional analysis strongly suggest that OGG1 is responsible for ROS protection in
467 GS cells.

468 While our results showed the importance of *Ogg1* in GS cells, *Ogg1* KO mice
469 do not show apparent spermatogenic defects despite increased 8-OxoG formation in
470 somatic tissues [53]. We think that culturing spermatogonia probably increases the

exposure to ROS because ROS are required for GS cell proliferation [9]. Because GS cells proliferate more actively than undifferentiated spermatogonia in vivo [4], GS cells probably depend more heavily on ROS than SSCs in vivo, which likely have less mutations. In this sense, it is probably not surprising that reproductive defects do occur in the descendants of triple compound *Ogg1*/*Mth1*/*Mutyh* mutants [54]. Because GS cells are exposed to high levels of ROS and they also divide faster than SSCs in vivo, it is likely that such conditions induce more mutations in the genome of GS cells. However, SSCs in vivo probably take longer periods to accumulate mutations. MTH1 degraded 8-OxodG in the nucleotide pool to prevent its incorporation into DNA, while MUTYH removed adenine misincorporated by replicative polymerases opposite the oxidized purine 8-OxoG. Interestingly, the triple KO mice were fertile but failed to produce progeny after eight generations. They exhibit an increased incidence of hydrocephaly and cancers, suggesting that these genes influence the frequency of de novo mutations in germ cells. Although the target cell type was not examined in that study, SSCs are most likely the best candidate cell because newly generated mutations in committed progenitors will disappear as they undergo only a limited number of cell divisions and complete spermatogenesis. SSCs are the only cells that can accumulate these mutations by self-renewal. Therefore, these results support our observation that BER enzymes, including OGG1, play critical roles in the protection of SSCs against ROS.

One of the important next questions is how OGG1 protects GS cells from ROS-induced damage. OGG1 translocated into the nucleus when high concentration of H_2O_2 was added to culture medium, which suggested that GS cells have a mechanism to

493 monitor and modulate ROS levels upon acute ROS-induced damages. Several anti-
494 oxidant molecules reportedly protect spermatogonia from ROS. For example,
495 spermatogonia express significantly high levels of NRF2 or SOD1 [55,56]. Because
496 animals lacking these molecules are extremely sensitive to ROS, it is likely that they share
497 a close relationship with OGG1. In fact, OGG1 is reportedly induced by NRF2 [57], and
498 *Sod1* OE decreases mutation frequency in Big Blue mice [58]. Therefore, these molecules
499 likely create a network of ROS defenses. The next important step is to clarify the
500 relationships among these molecules, which will lead to a better understanding of the
501 mechanism by which ROS allow self-renewal without damaging the genome of SSCs.
502 Our study shows that GS cells depend on OGG1 to protect their genome from
503 ROS. Although we still do not know the long-term impact and phenotype of abnormal
504 *Ogg1* expression, this can be examined using transplantation assay of Big Blue GS cells
505 after overexpression or KD. Understanding the degree of DNA damage in SSCs is
506 important for future clinical applications of SSCs for male infertility treatment [59],
507 because increased mitosis during culture may give rise to undesired de novo mutations,
508 which has been a concern for regenerative medicine [60]. Thus, the analysis of DNA
509 mutation patterns and understanding the mechanism of BER activity in SSCs have
510 important implications in not only understanding the mechanism of the self-renewal
511 process, but also for understanding disease etiology and for developing future
512 applications in medicine.
513

514 **Acknowledgments**

We thank Ms. S. Ikeda for technical assistance, and Dr. H. Sasanuma for helpful discussion.

References

1. Vitale I, Manic G, De Maria R, Kroemer G, Galluzzi L. DNA damage in stem cells. Mol Cell 2017;66:306-319.
2. Walter CA, Intano GW, McCarrey JR, McMahan A, Walter RB. Mutation frequency declines during spermatogenesis in young mice but increases in old mice. Proc Natl Acad Sci USA 1998;*95*: 10015-10019.
3. Wilson-Sayres MA, Makova KD. Genome analyses substantiate male mutation bias in many species. Bioessays 2011;33: 938-945.
4. de Rooij DG. The nature and dynamics of spermatogonial stem cells. Development 2017;144:3022-3030.
5. Meistrich, M.L., and van Beek, M.E.A.B. (1993). Spermatogonial stem cells. In Cell and molecular biology of the testis, C.C. Desjardins, and L.L. Ewing, ed. (Cambridge, UK: Oxford University Press), pp. 266-295.
6. Tegelenbosch RAJ, de Rooij DG. A quantitative study of spermatogonial multiplication and stem cell renewal in the C3H/101 F1 hybrid mouse. Mutat Res 1993;290:193-200.
7. Kanatsu-Shinohara M, Ogonuki N, Inoue K, Miki H, Ogura A, Toyokuni S, Shinohara T. Long-term proliferation and germline transmission of mouse male germline stem cells. Biol Reprod 2003;69: 612-616.

8. Kanatsu-Shinohara M, Shinohara T. Spermatogonial stem cell self-renewal and development. Annu Rev Cell Dev Biol 2013;29:163-187.
9. Morimoto H, Iwata K, Ogonuki N, Inoue K, Ogura A, Kanatsu-Shinohara T, Morimoto T, Yabe-Nishimura C, Shinohara T. ROS are required for mouse spermatogonial stem cell self-renewal. Cell Stem Cell 2013;12:774-786.
10. Morimoto H, Kanatsu-Shinohara M, Ogonuki N, Kamimura S, Ogura A, Yabe-Nishimura C, Mori Y, Morimoto T, Watanabe S, Otsu K, et al. ROS amplification drives mouse spermatogonial stem cell self-renewal. Life Sci Alliance 2019;2: 2.
11. Mao Z, Bozzella M, Seluanov A, Gorbunova V. Comparison of nonhomologous end joining and homologous recombination in human cells. DNA Repair 2008;7:1765-1771.
12. Lu AL, Li X, Gu Y, Wright PM, Chang DY. Repair of oxidative DNA damage mechanisms and functions. Cell Biochem Biophys *2001;35: 1*41-170.
13. Rübe CE, Zhang S, Miebach N, Fricke A, Rübe C. Protecting the heritable genome: DNA damage response mechanism in spermatogonial stem cells. DNA Repair 2011;10:159-168.
14. Kohler SW, Provost GS, Fieck A, Kretz PL, Bullock WO, Sorge JA, Putman DL, Short JM. Spectra of spontaneous and mutagen-induced mutations in the lacI gene in transgenic mice. Proc Natl Acad Sci USA 1991;88:7958-7962.
15. Cooper DJ, Chen IC, Hernandez C, Wang Y, Walter CA, McCarrey JR. Pluripotent cells display enhanced resistance to mutagenesis. Stem Cell Res. 2017;19:113-117.
16. Murphey P, McLean DJ, McMahan CA, Walter CA, McCarrey JR. Enhanced genetic

559 integrity in mouse germ cells. Biol Reprod 2013;88: 6.
560 17. Ishii K, Ishiai M, Morimoto H, Kanatsu-Shinohara M, Niwa O, Takata M,
561 Shinohara T. The Trp53-Trp53inp1-Tnfrsf10b pathway regulates the radiation
562 response of mouse spermatogonial stem cells. Stem Cell Reports 2014;3:676-689.
563 18. Aladjem MI, Spike BT, Rodewald LW, Hope TJ, Klemm M, Jaenisch R, Wahl GM.
564 ES cells do not activate p53-dependent stress responses and undergo p53-independent
565 apoptosis in response to DNA damage. Curr Biol 1998;8:145-155.
566 19. Kanatsu-Shinohara M, Inoue K, Lee J, Yoshimoto M, Ogonuki N, Miki H, Baba S,
567 Kato T, Kazuki Y, Toyokuni S, et al. Generation of pluripotent cells from neonatal
568 mouse testis. Cell 2004;119:1001-1012.
569 20. Takashima S, Hirose M, Ogonuki N, Ebisuya M, Inoue K, Kanatsu-Shinohara M,
570 Tanaka T, Nishida E, Ogura A, Shinohara T. Regulation of pluripotency in male
571 germline stem cells by Dmrt1. Genes Dev 2013;27:1949-1958.
572 21. Kanatsu-Shinohara M, Ogonuki N, Matoba S, Morimoto H, Ogura A, Shinohara T.
573 Improved serum- and feeder-free culture of mouse spermatogonial stem cells. Biol
574 Reprod 2014;91:88.
575 22. Tsuda M, Cho K, Ooka M, Shimizu N, Watanabe R, Yasui A, Nakazawa Y, Ogi T,
576 Harada H, Agama K, et al. ALC1/CHD1L, a chromatin-remodeling enzyme, is
577 required for efficient base excision repair. PLoS One 2017;12: e0188320.
578 23. Agresti A. Categorical Data Analysis. 2002; Wiley, New York.
579 24. Fay M. Two-sided Exact Tests and Matching Confidence Intervals for Discrete Data.
580 R Journal. 2010;2/1, 53–58.

581 25. Hirji K. Exact Analysis of Discrete Data. 2006; Chapman and Hall/CRC; New York.
582 ISBN: 142003619X, 9781420036190.
583 26. Kanatsu-Shinohara M, Toyokuni S, Shinohara T. CD9 is a surface marker on mouse
584 and rat male germline stem cells. Biol Reprod 2004;70: 70-75.
585 27. Lieber MR, Hesse JE, Mizuuchi K, Gellert M. Developmental stage specificity of the
586 lymphoid V(D)J recombination activity. Genes Dev. 1987;1: 751-761.
587 28. Arad U. Modified Hirt procedure for rapid purification of extrachromosomal DNA
588 from mammalian cells. Biotechniques 1998; 24:760-762.
589 29. Pierce AJ, Johnson RD, Thompson LH, Jasin M. XRCC3 promotes homology-
590 directed repair of DNA damage in mammalian cells. Genes Dev 1999;13: 2633-2638.
591 30. Sakamoto S, Iijima K, Mochizuki D, Nakamura K, Teshigawara K, Kobayashi J,
592 Matsuura S, Tauchi H, Komatsu K. Homologous recombination repair is regulated by
593 domains at the N- and C-terminus of NBS1 and is dissociated with ATM mutations.
594 Oncogene 2007;*26*:6002-6009.
595 31. Singh NP, McCoy MT, Tice RR, Schneider EL. A simple technique for quantitation
596 of low levels of DNA damage in individual cells. Exp. Cell Res. 1998;175:184-191.
597 32. Tsuda H. Chromosomal aberrations induced by hydrogen peroxide in cultured
598 mammalian cells. Jpn J Genet 1981;56, 1-8.
599 33. Stambrook PJ, Tichy ED. Preservation of genomic integrity in mouse embryonic stem
600 cells. Adv Exp Med Biol 2010;695: 59-75.
601 34. Intano GW, McMahan CA, Walter RB, McCarrey JR, Walter CA. Mixed
602 spermatogenic germ cell nuclear extracts exhibit high base excision repair activity.

603 Nucleic Acids Res 2001; 29:1366-1372.
604 35. Mahjabeen I, Chen Z, Zhou X, Kayani MA. Decreased mRNA expression levels of
605 base excision repair (BER) pathway genes is associated with enhanced Ki-67
606 expression in HNSCC. Med Oncol 2012;29: 3620-3625.
607 36. Yamamoto M, Yamamoto R, Takenaka S, Matsuyama S, Kubo K. Abundance of
608 BER-related proteins depends on cell proliferation status and the presence of DNA
609 polymerase β. J Radiat Res 2015;56: 607-614.
610 37. Wood RD, Mitchell M, Sgouros J, Lindahl T. Human DNA repair genes. Science
611 2001;291: 1284-1289.
612 38. Lin Z, Zhang X, Tuo J, Guo Y, Green B, Chan CC, Tan W, Huang Y, Ling W, Kadlubar
613 FF, Lin D, Ning B. A variant of the Cockayne syndrome B gene ERCC6 confers risk
614 of lung cancer. Hum Mutat 2008;29: 113-122.
615 39. Hegde ML, Theriot CA, Das A, Hegde PM, Guo Z, Gary RK, Hazra TK, Shen B,
616 Mitra S. Physical and functional interaction between human oxidized base-specific
617 DNA glycosylase NEIL1 and flap endonuclease 1. J Biol Chem 2008;283: 27028-
618 27037.
619 40. Liu T, Huang J. Replication protein A and more: single-stranded DNA-binding
620 proteins in eukaryotic cells. Acta Biochim Biophys Sin (Shanghai) 2016;48: 665-670.
621 41. Ba X, Boldogh I. 8-Oxoguanine DNA glycosylase 1: Beyond repair of the oxidatively
622 modified base lesions. Redox Biol 2018;14:669-678.
623 42. Campalans A, Amouroux R, Bravard A, Epe B, Radicella J. UVA irradiation induces
624 relocalisation of the DNA repair protein hOGG1 to nuclear speckles. J Cell Sci 2007;

120:23-32.

43. Johnston DS, Wright WW, DiCandeloro P, Wilson E, Kopf GS, Jelinsky SA. Stage-specific gene expression is a fundamental characteristics of rat spermatogenic cells and Sertoli cells. Proc Natl Acad Sci USA 2008;105:8315-8320.
44. Iwamori N, Iwamori T, Matzuk MM. Characterization of spermatogonial stem cells lacking intercellular bridges and genetic replacement of a mutation in spermatogonial stem cells. PLoS One 2012; 7:e38914.
45. Kanatsu-Shinohara M, Ikawa M, Takehashi M, Ogonuki N, Miki H, Inoue K, Kazuki Y, Lee J, Toyokuni S, Oshimura M, et al. Production of knockout mice by random or targeted mutagenesis in spermatogonial stem cells. Proc Natl Acad Sci USA 2006; 103:8018-8023.
46. Kanatsu-Shinohara M, Kato-Itoh M, Ikawa M, Takehashi M, Sanbo M, Morioka Y, Tanaka T, Morimoto H, Hirabayashi M, Shinohara T. Homologous recombination in rat germline stem cells. Biol Reprod 2011; 85:208-217.
47. Kashiwagi H, Shiraishi K, Sakaguchi K, Nakahama T, Kodama S. Repair kinetics of DNA double-strand breaks and incidence of apoptosis in mouse neural stem/progenitor cells and their differentiated neurons exposed to ionizing radiation. J Radiat Res 2018; 59:261-271.
48. Kass EM, Helgadottir HR, hen CC, Barbera M, Wang R, Westermark UK, Ludwig T, Moynahan ME, Jasin M. Double-strand break repair by homologous recombination in primary mouse somatic cells require BRCA1 but not the ATM kinase. Proc Natl Acad Sci USA 2013;110:5564-5569.

647 49. Huamari J, McMahan CA, Herbert DC, Reddick R, McCarrey JR, Maclnnes MI,
648 Chen DJ, Walter CA. Spontaneous mutagenesis is enhanced in Apex heterozygous
649 mice. Mol Cell Biol 2004; 24:8145-8153.
650 50. Vogel KS, Perez M, Momand JR, Acevedo-Torres K, Hildreth K, Garcia RA, Torres-
651 Ramos CA, Ayala-Torres S, Prihoda TJ, McMahan CA, et al. Age-related instability
652 in spermatogenic cell nuclear and mitochondrial DNA obtained from Apex1
653 heterozygous mice. Mol Reprod Dev 2011; 78: 906-919.
654 51. Intano GW, McMahan CA, McCarrey JR, Walter RB, McKenna AE, Matsumoto Y,
655 Maclnnes MA, Chen DJ, Walter CA. Base excision repair is limited by different
656 proteins in male germ cell nuclear extracts prepared from young and old mice. Mol
657 Cell Biol 2002; 22:2410-2418.
658 52. Klungland A, Bjelland S. Oxidative damage to purines in DNA: Role of mammalian
659 Ogg1. DNA Repair 2007; 6:481-488.
660 53. Minowa O, Arai T, Hirano M, Monden Y, Nakai S, Fukuda M, Itoh M, Takano H,
661 Hippou Y, Aburatani H, et al. Mmh/Ogg1 gene inactivation results in accumulation
662 of 8-hydroxyguanine in mice. Proc Natl Acad Sci U S A 2000; 97:4156-61.
663 54. Ohno M, Sakumi K, Fukumura R, Furuichi M, Iwasaki Y, Hokama M, Ikemura T,
664 Tsuzuki T, Gondo Y, Nakabeppu Y. 8-oxoguanine causes spontaneous de novo
665 germline mutations in mice. Sci Rep 2014;4: 4689.
666 55. Ishii T, Matsuki S, Iuchi Y, Okada F, Toyosaki S, Tomita Y, Ikeda Y, Fujii J.
667 Accelerated impairment of spermatogenic cells in sod1-knockout mice under heat
668 stress. Free Radic Res 2005; 39:697-705.

669 56. Nakamura BN, Lawson G, Chan JY, Banuelos J, Cortes MM, Hoang YD, Ortiz L,
670 Rau BA, Luderer U. Knockout of the transcription factor NRF2 disrupts
671 spermatogenesis in an age-dependent manner. Free Radic Biol Med 2010; 49:1368-
672 1379.
673 57. Singh B, Chatterjee A, Ronghe A, Bhat NK, Bhat HK. Antioxidant-mediated up-
674 regulation of OGG1 via NRF2 induction is associated with inhibition of oxidative
675 DNA damage in estrogen-induced breast cancer. BMC Cancer 2013; 13:253.
676 58. Kunishige M, Hill KA, Riemer AM, Farwell KD, Halangoda A, Heinmöller E, Moore
677 SR, Turner DM, Sommer SS. Mutation frequency is reduced in the cerebellum of Big
678 Blue mice overexpressing a human wild type SOD1 gene. Mutat Res 2001; 473:139-
679 149.
680 59. Mulder CL, Zheng Y, Jan SZ, Struijk RB, Repping S, Hamer G, van Pelt AM.
681 Spermatogonial stem cell autotransplantation and germline genome editing: a future
682 cure for spermatogenic failure and prevention of transmission of genomic diseases.
683 Hum Reprod Update 2016; 22:561-573.
684 60. Liang G, Zhang Y. Genetic and epigenetic variations in iPSCs: potential causes and
685 implications for application. Cell Stem Cell 2013; 13:149-159.

686

687 **Figure legends**

688

689 Figure 1. Enhanced resistance of GS cells to ROS.

690 (A) Appearance of different types of cells cultured with H_2O_2. Cells were maintained for
691 6 days. Scale bar, 50 μm.
692 (B) Survival rate of H_2O_2-treated cells. GS cells were cultured for 6 days, while the other
693 cell types were recovered 3 days after culture initiation because they proliferate more
694 quickly (mean ± SEM, n = 6). Results of three experiments. Significantly more GS cells
695 survived compared to other cell types. *P < 0.05.
696 (C) TUNEL staining. GS cells were analyzed 6 days after culture, whereas the rest of the
697 cells were analyzed at 3 days. At least 150 cells were counted. Results of three
698 experiments. Scale bar, 50 μm. Counterstained by Hoechst 33342**.** *P < 0.05.
699 (D) Comet assay. Each cell type was exposed to different doses of H_2O_2 for 30 min and
700 then incubated in normal media for indicated periods. The cells were then electroporated
701 and stained with ethidium bromide. The head (round shape) corresponds to undamaged
702 DNA while the tail (smear) corresponds to damaged DNA. At least 40 cells were picked
703 up and the intensity ratio of head over total DNA was quantified. Results of two
704 experiments. This experiment was replicated three times. *P < 0.05.
705
706 Figure 2. Repair of DSBs in GS cells.
707 (A) Real-time PCR analyses of genes involved in DSB repair (mean ± SEM, n = 4).
708 (B) Experimental scheme of NHEJ assay using pJH200 substrate vector and *Rag1/2*
709 expressing plasmids. pJH200 and *Rag1/2* were cotransfected (i). RAG1/2 cut both sides
710 of the stop codon (ii). NHEJ machinery facilitates joining of the blunt ends and the

711 construct was introduced into *E.Coli* (iii). Colonies were counted whose number
712 represents the efficacy of successful NHEJ (iv).
713 (C) Quantification of colonies (mean ± SEM, n = 5). NHEJ ratio was measured by
714 dividing the colony numbers on Amp^+/Cm^+ plates by those on Amp^+ plates. The number
715 on Amp^+ plates reflects transfection efficiency. Results of five experiments. *$P < 0.05$.
716 (D) Experimental scheme of the HR assay using the pHPRT-DRGFP plasmid. DRGFP
717 contains two incomplete GFP sequences (i). DRGFP, *DsRed*, and *Sce-I* were transfected
718 into GS and ES cells. *SCE-I* cut the target sequence in the GFP sequence and DsRed was
719 used as a control for measuring transfection efficiency (ii). Recombination occurred
720 between the two incomplete GFP sequences (iii). The resultant GFP had a complete
721 sequence for emitting fluorescence (iv).
722 (E) Flow cytometric analyses of transfected cells (mean ± SEM, n = 5). Results of two
723 experiments. Y-axis indicates the ratio of GFP^+ $DsRed^+$ population over $DsRed^+$
724 population. Successful recombination of pHPRT-DRGFP yields green fluorescence and
725 DsRed is used to estimate transfection efficiency.
726
727 Figure 3. Big Blue assay of GS cells.
728 (A) Experimental scheme of Big Blue assay. Each cell type was collected from Big Blue
729 mice carrying the *LacI* transgene (i). Genomic DNA was extracted from Big Blue cells
730 (ii), and packaged into a lambda phage (iii), which infected *E. coli* (iv). The ratio of blue
731 and white plaque numbers was determined (v).

732 (B) Mutation frequency. Plaque forming unit (Pfu) stands for the total number of plaques
733 counted. The *LacI* transgene from blue plaque was sequenced to confirm the
734 independency of each mutation. For 2.5M-GS cells, one of the 8 mutant plaques showed
735 two different mutations, and 9 independent mutations were found via sequencing. Since
736 the sequence change was different for each of these mutations, we counted them as 2
737 unique, independent mutations in this case. NA, not applicable because cells were not
738 cultured.
739
740 Figure 4. Impaired GS cell proliferation by *Ogg1* depletion.
741 (A) Real-time PCR analyses of BER-related genes (mean ± SEM, n = 4). Results of two
742 experiments. *P < 0.05.
743 (B) Cell recovery after transfection of shRNA against indicated genes 6 days after
744 transfection (mean ± SEM, n = 6). Results of two experiments. *P < 0.05.
745 (C) Western blotting analyses of OGG1 in GS cells (mean ± SEM, n = 6). Results of three
746 experiments. *P < 0.05.
747 (D) Immunostaining of OGG1 and spermatogenic markers. Cells in 35 tubules were
748 counted. Scale bar, 20 μm. Counterstained by Hoechst 33342. *P < 0.05.
749
750 Figure 5. Impact of *Ogg1* on H_2O_2 resistance of GS cells.
751 (A) Comet assay. GS cells were transfected with shRNA or cDNA and analyzed 2 days
752 after transfection. Cells were then exposed to H_2O_2 (500 μM) for 30 min followed by

753 recovery at indicated time points. At least 30 cells were counted for each cell type (mean
754 ± SEM). Results of two experiments. *P < 0.05.
755 (B) Experimental scheme of H_2O_2 resistance analyses. GS cells were transfected with
756 shRNA, and half of the transfected cells were exposed to H_2O_2 (200 μM). The ratio of
757 cells that survived [cells with H_2O_2 (a)/cells without H_2O_2 (b)] was determined 6 days
758 after transfection.
759 (C) Survival of GS cells after *Ogg1* OE (n = 7)/KD (n = 6)(mean ± SEM). The ratio of
760 cells that survived [cells with H_2O_2 (a)/cells without H_2O_2 (b)] in (B) was determined in
761 at least 2 independent experiments 6 days after transfection.
762 (D) Immunostaining of OGG1 in GS cells 1 day after H_2O_2 exposure (mean ± SEM, n =
763 24). Results of two experiments. BF, bright field. Scale bar, 10 μm. Counterstained by
764 Hoechst 33342. *P < 0.05.

Figure 1

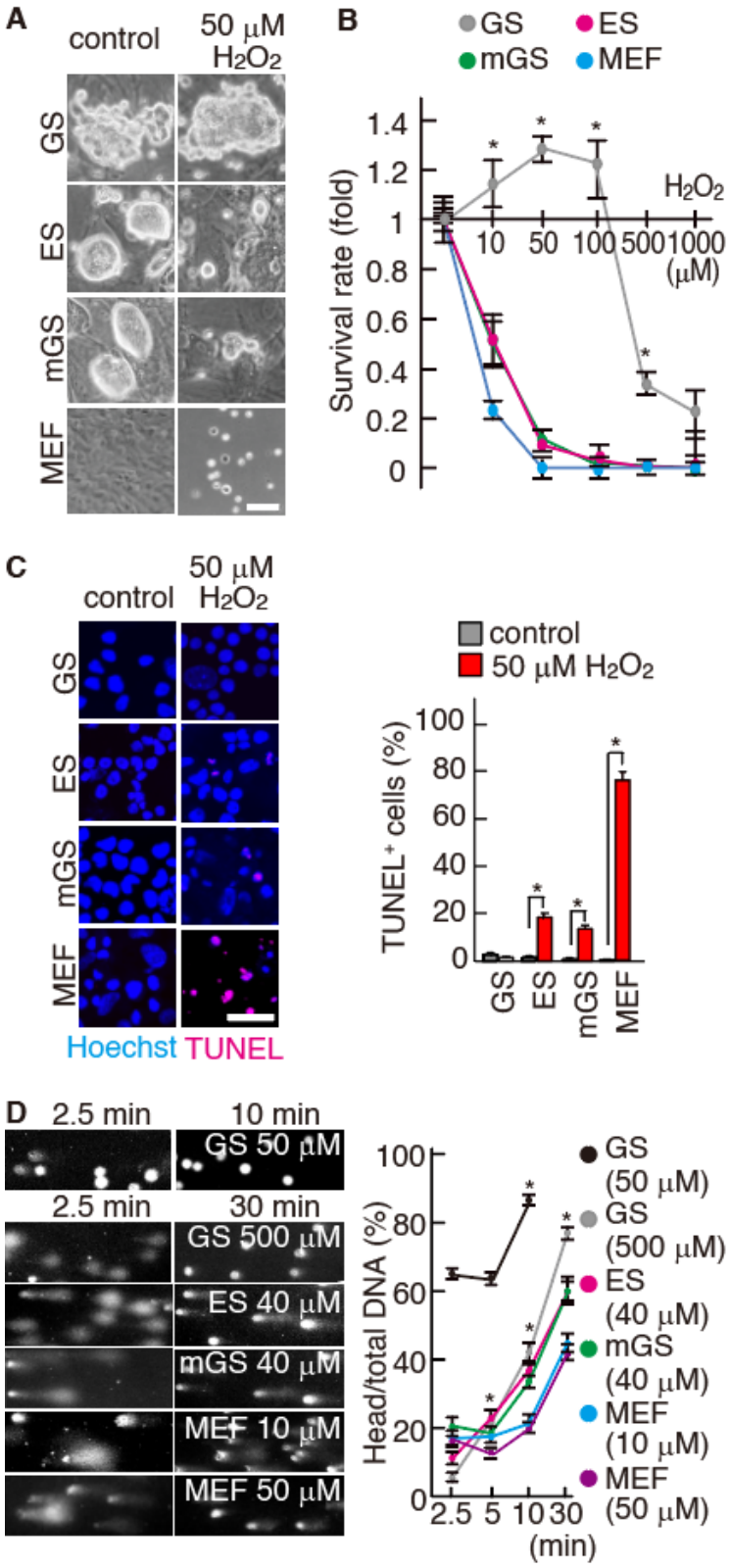
A
control
50 μM H2O2
GS
ES
mGS
MEF
B
GS
ES
mGS
MEF
Survival rate (fold)
H2O2
10 50 100 500 1000
(μM)
C
control
50 μM H2O2
Hoechst TUNEL
TUNEL+ cells (%)
D
2.5 min
10 min
GS 50 μM
2.5 min
30 min
GS 500 μM
ES 40 μM
mGS 40 μM
MEF 10 μM
MEF 50 μM
Head/total DNA (%)
GS (50 μM)
GS (500 μM)
ES (40 μM)
mGS (40 μM)
MEF (10 μM)
MEF (50 μM)
(min)

Figure 2

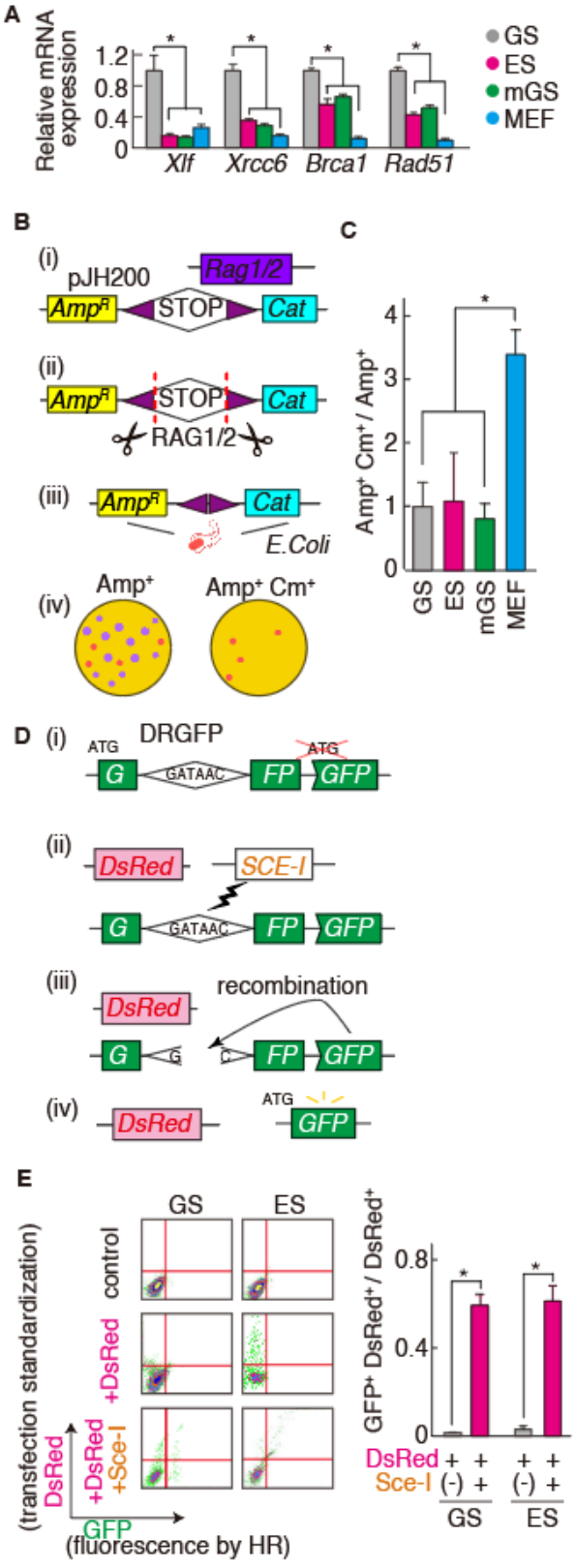
A
Relative mRNA expression
1.2
0.8
0.4
0
Xlf
Xrcc6
Brca1
Rad51
GS
ES
mGS
MEF
B
(i)
pJH200
Rag1/2
Amp^R
STOP
Cat
(ii)
RAG1/2
(iii)
E.Coli
(iv)
Amp+
Amp+ Cm+
C
Amp+ Cm+ / Amp+
GS
ES
mGS
MEF
D
(i)
DRGFP
ATG
G
GATAAC
FP
GFP
(ii)
DsRed
SCE-I
(iii)
recombination
(iv)
E
GS
ES
control
+DsRed
+DsRed +Sce-I
DsRed
GFP
(transfection standardization)
(fluorescence by HR)
GFP+ DsRed+ / DsRed+
DsRed
Sce-I
GS
ES

Figure 3

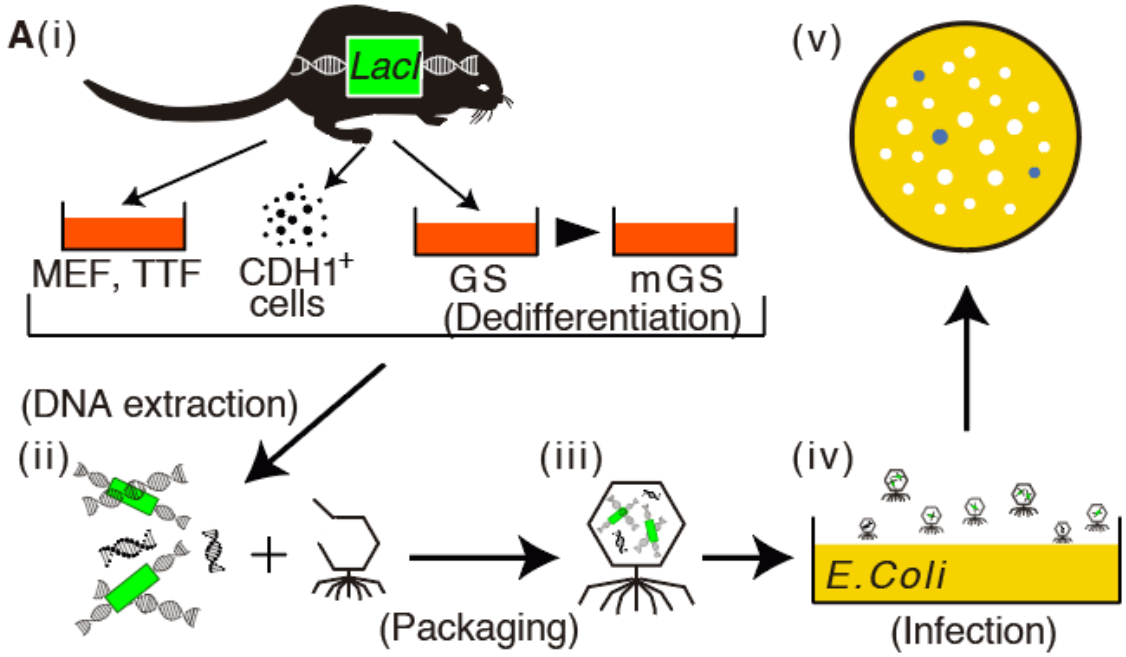

B

Cell-type	Doubling time (h)	Pfu number	Mutation number (before sequencing)	Independent mutation	Mutation frequency ($x10^{-5}$)
GS (8 mo)	75	1,213,368	5	5	0.41
GS (31 mo)	60	726,680	5	5	0.69
$CDH1^+$ (9±1 mo)	NA	363,052	7	7	1.93
mGS	23	362,943	20	6	1.65
MEF	30	136,682	11	10	7.32
TTF	132	51,471	10	10	19.43

Figure 4

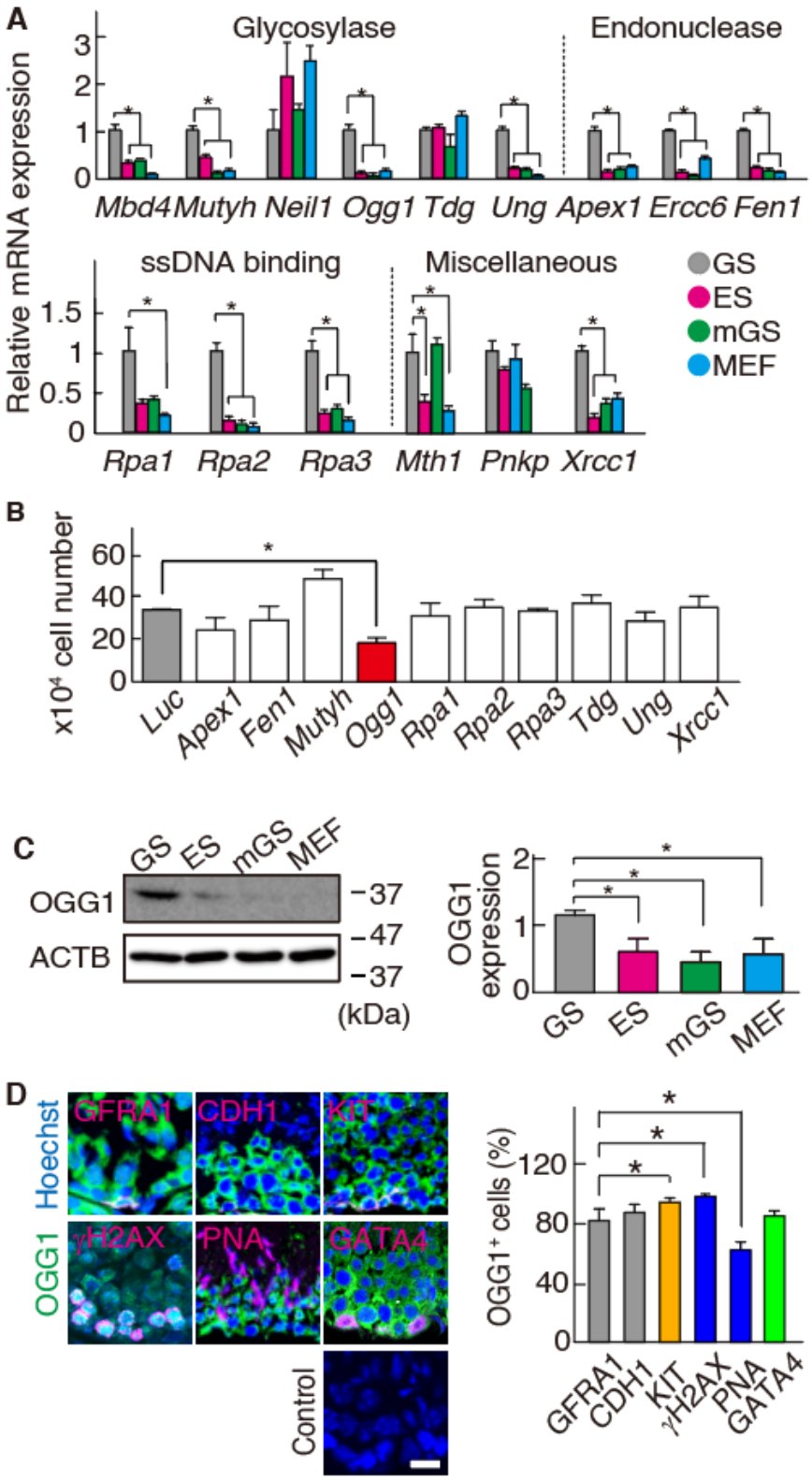
A
Glycosylase
Endonuclease
Relative mRNA expression
Mbd4 Mutyh Neil1 Ogg1 Tdg Ung Apex1 Ercc6 Fen1
ssDNA binding
Miscellaneous
GS
ES
mGS
MEF
Rpa1 Rpa2 Rpa3 Mth1 Pnkp Xrcc1
B
x10⁴ cell number
Luc Apex1 Fen1 Mutyh Ogg1 Rpa1 Rpa2 Rpa3 Tdg Ung Xrcc1
C
GS ES mGS MEF
OGG1
ACTB
37
47
37
(kDa)
OGG1 expression
D
Hoechst
OGG1
GFRA1
CDH1
KIT
γH2AX
PNA
GATA4
Control
OGG1⁺ cells (%)

Figure 5

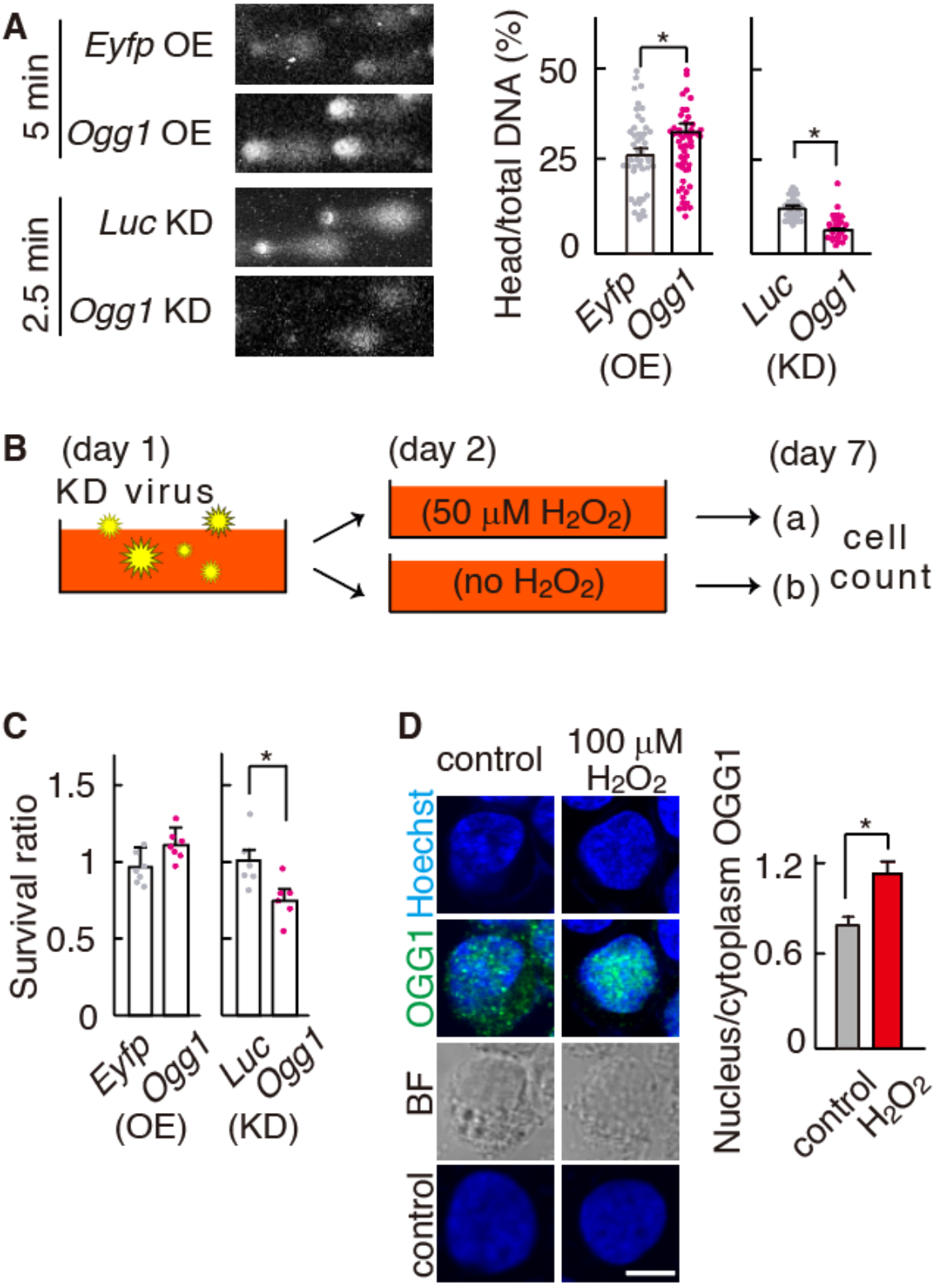
A
5 min
Eyfp OE
Ogg1 OE
2.5 min
Luc KD
Ogg1 KD
Head/total DNA (%)
50
25
0
*
*
Eyfp
Ogg1
Luc
Ogg1
(OE)
(KD)
B
(day 1)
KD virus
(day 2)
(50 μM H2O2)
(no H2O2)
(day 7)
(a)
(b)
cell count
C
Survival ratio
1.5
1
0.5
0
*
Eyfp
Ogg1
Luc
Ogg1
(OE)
(KD)
D
control
100 μM H2O2
OGG1 Hoechst
BF
control
Nucleus/cytoplasm OGG1
1.2
0.6
0
*
control
H2O2